Research Paper

The Holocene
2021, Vol. 31(8) 1288–1303
© The Author(s) 2021
Article reuse guidelines:
sagepub.com/journals-permissions
DOI: 10.1177/09596836211011656
journals.sagepub.com/home/hol
SAGE

Climate-induced treeline mortality during the termination of the Little Ice Age in the Greater Yellowstone Ecoregion, USA

Maegen L Rochner,[1] Karen J Heeter,[2] Grant L Harley,[2] Matthew F Bekker[3] and Sally P Horn[4]

Abstract

Paleoclimate reconstructions for the western US show spatial variability in the timing, duration, and magnitude of climate changes within the Medieval Climate Anomaly (MCA, ca. 900–1350 CE) and Little Ice Age (LIA, ca. 1350–1850 CE), indicating that additional data are needed to more completely characterize late-Holocene climate change in the region. Here, we use dendrochronology to investigate how climate changes during the MCA and LIA affected a treeline, whitebark pine (*Pinus albicaulis* Engelm.) ecosystem in the Greater Yellowstone Ecoregion (GYE). We present two new millennial-length tree-ring chronologies and multiple lines of tree-ring evidence from living and remnant whitebark pine and Engelmann spruce (*Picea engelmannii* Parry ex. Engelm.) trees, including patterns of establishment and mortality; changes in tree growth; frost rings; and blue-intensity-based, reconstructed summer temperatures, to highlight the terminus of the LIA as one of the coldest periods of the last millennium for the GYE. Patterns of tree establishment and mortality indicate conditions favorable to recruitment during the latter half of the MCA and climate-induced mortality of trees during the middle-to-late LIA. These patterns correspond with decreased growth, frost damage, and reconstructed cooler temperature anomalies for the 1800–1850 CE period. Results provide important insight into how past climate change affected important GYE ecosystems and highlight the value of using multiple lines of proxy evidence, along with climate reconstructions of high spatial resolution, to better describe spatial and temporal variability in MCA and LIA climate and the ecological influence of climate change.

Keywords

dendrochronology, Greater Yellowstone, Little Ice Age, treeline, whitebark pine

Received 3 November 2020; revised manuscript accepted 4 March 2021

Introduction

Summer temperatures are the primary driver of tree growth at both high latitudes and high elevations (Fritts, 2001; Kauppi and Posch, 1985; Rossi et al., 2008), and with ongoing climate change these locations are expected to experience the greatest temperature increases in the future (IPCC, 2013; Mountain Research Initiative EDW Working Group, 2015). Consequences of this warming include northward and upward shifts in the ranges of plant species (Grace et al., 2002; Holtmeier and Broll, 2005; Körner, 2003; Schwörer et al., 2017), and altered treeline composition and structure because of changes in growth, recruitment, and population density of component tree species (MacDonald et al., 1998). These ecological changes can subsequently impact ecosystem services, microclimates, biodiversity, and at some scales, surface energy budgets and related climate feedbacks (MacDonald et al., 1998; Schwörer et al., 2017; Smith et al., 2009). One avenue for better understanding the potential effects of ongoing warming is to examine how treeline ecosystems have responded to climate change in the past.

In the Greater Yellowstone Ecoregion (GYE) and western United States (US), researchers have used paleoenvironmental records to examine Holocene climate change and shifts in forest composition. Treeline advance and other post-glacial changes during the early-to-middle Holocene, including during the warmer Climate Optimum from ca. 9000–5000 cal yr BP, have been documented using evidence in lake-sediment cores (e.g. pollen, charcoal, wood fragments, conifer needles) from the Wind River Range of northwestern Wyoming (Fall et al., 1995; Lynch, 1998), the Snowy Range of southeastern Wyoming (Mensing et al., 2012), and Yellowstone and Grand Teton National Parks (Krause and Whitlock, 2013; Krause et al., 2015; Whitlock, 1993). Additional studies in the western US used radiocarbon and tree-ring dates from subfossil wood to document higher-than-present treelines during intervals of the Holocene, including for the White Mountains of California (LaMarche, 1973; LaMarche and Mooney, 1967, 1972; Salzer et al., 2014), the Snake Range of Nevada (LaMarche and Mooney, 1967; Salzer et al., 2014), the

---

[1]Department of Geography and Geosciences, The University of Louisville, Louisville, Kentucky, USA
[2]Department of Geography and Geological Sciences, University of Idaho, Moscow, Idaho, USA
[3]Department of Geography, Brigham Young University, Provo, Utah, USA
[4]Department of Geography, The University of Tennessee, Knoxville, Tennessee, USA

Corresponding author:
Maegen L Rochner, Geography and Geosciences, University of Louisville, 219 Lutz Hall, Louisville, KY 40292, USA.
Email: maegen.rochner@louisville.edu

Ruby Mountains of Nevada (Salzer et al., 2014), the Rocky Mountain Front Range of Colorado (Carrara and McGeehin, 2015), the Sierra Nevada of California (Lloyd and Graumlich, 1997; Scuderi, 1987), and the Wind River Range of Wyoming (Morgan et al., 2014). Missing from, or incomplete within many of these records, however, is evidence of the influence of important climate changes of the late-Holocene, specifically the Medieval Climate Anomaly (MCA) and the Little Ice Age (LIA), on important treeline ecosystems.

The MCA (*ca*. 900–1350 CE) has been characterized as a period of anomalous warmth in the Northern Hemisphere (Bradley et al., 2003; Crowley and Lowery, 2000; Mann et al., 2009; Reinemann et al., 2014), but the duration, magnitude, and spatial patterns of warming are debated (Crowley, 2000; Crowley and Lowery, 2000; Reinemann et al., 2014). In contrast, the LIA (*ca*. 1350–1850 CE) was a period punctuated by decadal to multi-century-scale cooling events in the Northern Hemisphere, largely attributed to solar and volcanic forcing (Anchukaitis et al., 2017; Crowley, 2000; Crowley et al., 2008; Wagner and Zorita, 2005; Wanner et al., 2008; Wilson et al., 2016). In the western US, a series of prolonged droughts from 900 to 1300 CE occurred during the MCA (Coats et al., 2016; Cook et al., 2004; Herweijer et al., 2007; Stine, 1994), followed by generally cooler and wetter conditions and glacial advances during the LIA (Carrara, 1989; Luckman, 2000; Marcott et al., 2009; Osborn and Gerloff, 1997; Wiles et al., 2004). Spatial variability in the timing, duration, and magnitude of change during the MCA and LIA documented by dendroclimatological studies in the northern US and Canadian Rocky Mountains (Biondi et al., 1999; Kipfmueller, 2008; Luckman, 2000; Luckman and Wilson, 2005) indicates that additional studies are needed to more completely characterize these climate periods in the western US.

Millennial-length paleoenvironmental records are needed to capture both climate and ecological change during the MCA and LIA but are limited in the western US and GYE. Few of the lake-sediment based paleoclimate studies for the GYE have detected treeline changes during the MCA or LIA; researchers have instead concluded that modern treeline established by 5750–3000 cal. yr. BP based on pollen assemblages (Mensing et al., 2012; Whitlock, 1993). In the western US, studies of paleoclimate from remnant wood have shown wide variability in the timing of treeline advance and decline. A few documented higher-than-present treelines that predate the MCA by hundreds to over 1000 years (Carrara and McGeehin, 2015; LaMarche and Mooney, 1967, 1972) or indicated that higher-than-present treelines declined into and during the early MCA (LaMarche, 1973; Lloyd and Graumlich, 1997; Salzer et al., 2014; Scuderi, 1987). Only two studies have documented changes specific to the MCA and LIA. In the Sierra Nevada of California, Lloyd and Graumlich (1997) determined that treeline had experienced two declines in the last 1000 years, one during the MCA attributed to drought stress and another during the LIA attributed to cooling. Morgan et al. (2014) also documented treeline decline during the MCA, based on radiocarbon dating of remnant trees in the Wind River Range of Wyoming. In the GYE, paleoclimate data in lake sediment cores from Yellowstone National Park have provided evidence of MCA and LIA climate and environmental change, although not treeline change (Bracht et al., 2008; Meyer et al., 1992; Pierce et al., 2004). Studies of alluvial stratigraphy indicated increased fire-related sedimentation during warmer and drier periods, including the MCA, and decreased fire-related sedimentation and increased erosion under cooler and wetter conditions of the LIA (Meyer et al., 1992; Pierce et al., 2004). Shifting diatom assemblages in a sediment core from Crevice Lake, Yellowstone National Park, indicated changes in temperature and wind strength, which affected isothermal mixing and nutrient recycling during the transition from the MCA to the LIA (Bracht et al., 2008). While these data provide evidence of MCA and LIA climate changes in the GYE, they lack the resolution to examine spatial and especially temporal variability. Millennial-length tree-ring records, which remain quite rare for North America in general (Anchukaitis et al., 2017; Wilson et al., 2016), have the potential through annual resolution to not only inform variability within longer-term climate changes, but to provide multiple lines of proxy evidence for the impact of these changes on important ecosystems.

While knowledge of the MCA and LIA are incomplete in the GYE, this ecoregion is also of particular interest in the western US because it contains important treeline species and environments under threat from ongoing climate change. An improved understanding of late-Holocene climate will help to clarify the climatological and ecological history of the region, providing context for modern changes. Here, we use dendrochronological analyses of living and remnant whitebark pine (*Pinus albicaulis* Engelm.) and Engelmann spruce (*Picea engelmanni*i Parry ex Engelm.) trees to examine the influence of late-Holocene climate change, specifically during the MCA and LIA, on tree growth and temporal patterns of establishment and mortality in a treeline, whitebark pine ecosystem in the GYE. The objectives of this work were (1) to develop two new millennial-length tree-ring chronologies for whitebark pine and Engelmann spruce, rare for both studied species and for the northwestern US, (2) to reconstruct summer temperatures for the late LIA, and (3) to examine temporal patterns of growth, establishment, and mortality in relation to MCA and LIA climate changes. Results provide important insight into how past climate change affected important GYE ecosystems and highlight the value of using multiple lines of proxy evidence, along with climate reconstructions of high spatial resolution, to better describe spatial and temporal variability in MCA and LIA climate and the ecological influence of climate change.

Methods

Study site

Fantan Lake (FTL; 44.926 °N, 109.544 °W, 2800–3020 m elevation), located near the Beartooth Highway (US Highway 212) in the Shoshone National Forest (Figure 1), is a mixed subalpine ecosystem near treeline (3100–3200 m). The site is characterized by alpine meadows and clusters, or "islands," of whitebark pine, Engelmann spruce, and subalpine fir (*Abies lasiocarpa* (Hook.) Nutt.) trees, which tend to concentrate on outcrops of Precambrian granite and metamorphic rocks (Lageson and Spearing, 1991). We selected the site primarily because of the presence of large (approximately 70–90 cm diameter) whitebark pine and Engelmann spruce remnants, both scattered within the living tree islands and isolated in the alpine meadow (Figure 1). None of the living trees in the same area (average 38.6 cm diameter) rivaled the size of the remnant trees. This pattern suggested a significant mortality event that killed a mature, ancient forest and occurred recently enough that this forest has not been replaced by similarly aged trees. Additionally, many of the remnant trees still had intact outer rings. This combination of unique site features presented a prime opportunity to examine patterns of past climate and environmental change, as well as to provide historical insight and context for future changes in the ecosystem.

Sample preparation and chronology development

We targeted living, mature whitebark pine and Engelmann spruce trees from a variety of age groups at FTL to capture both the earliest and more recent periods of establishment. From selected whitebark pine and Engelmann spruce trees, we collected at least two increment cores as close to the root interface as possible to obtain the maximum number of growth rings and increase dating accuracy for individual trees (Stokes and Smiley, 1996). We

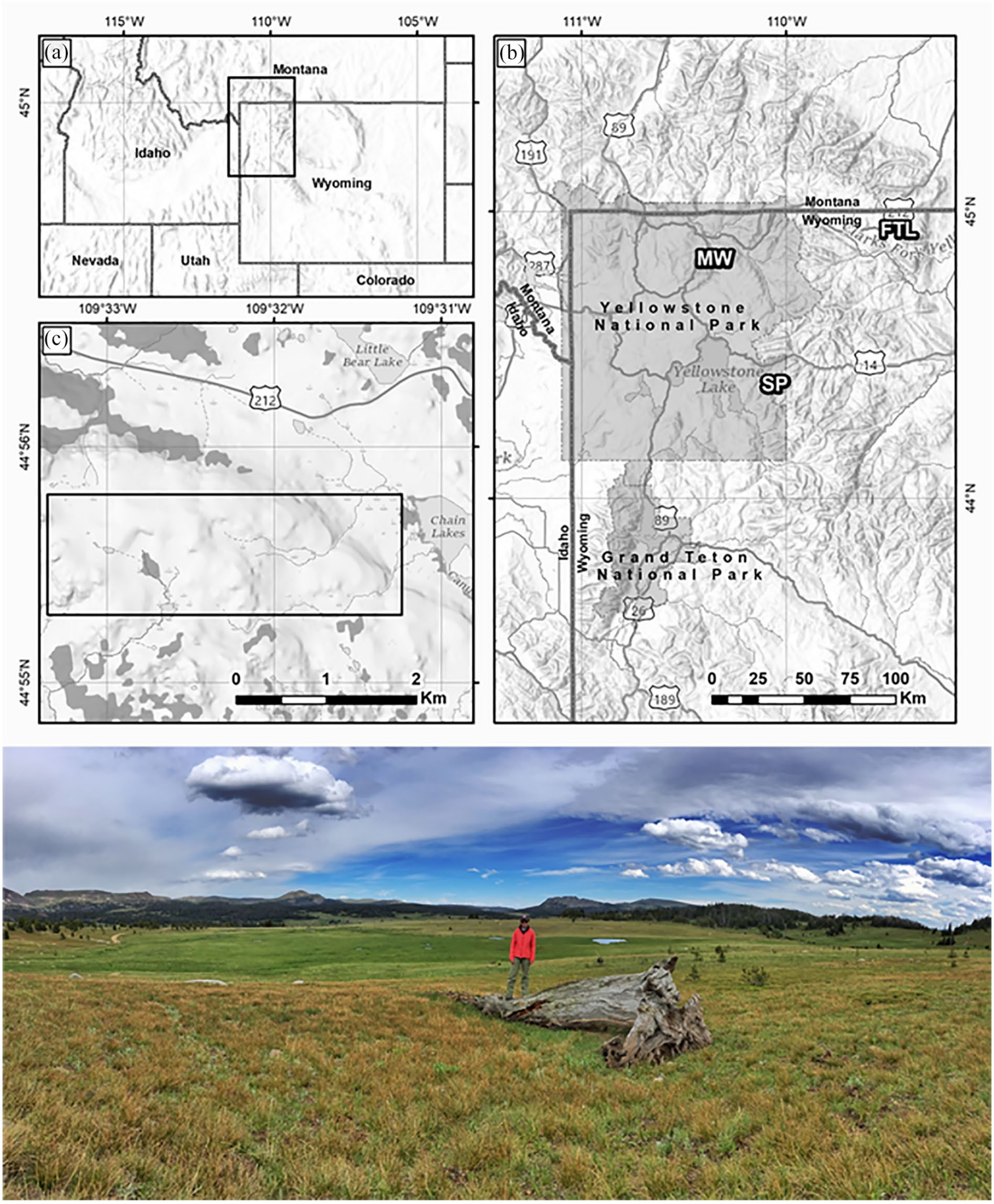

Figure 1. (a) Regional setting for the Greater Yellowstone, (b) Greater Yellowstone and locations of the FTL study site and the Mount Washburn (MW) and Sylvan Pass (SP) reference chronologies, (c) The FTL study site, delineated by black box, with more continuous woodland-type landcover represented by gray shading, and (bottom) author M. Rochner for scale of remnant sample found in alpine meadow. Map prepared by Donald J. Biddle of the University of Louisville Center for GIS. Data Citation: USGS: The National Map: National Hydrography Dataset and National Transportation Dataset; ESRI: USA Federal Lands; USGS Land Cover – Woodland for Wyoming 20160525 State or Territory Shapefile; ESRI: World Hillshade Map Service; USGS Land Cover – Woodland for Wyoming 20160525 State or Territory Shapefile; U.S. Census Bureau.

collected at least one cross section or wedge from all apparently intact remnant trees, including standing dead trees, or snags, and discarded those samples that were too rotten or broken to analyze in the laboratory. We sanded all cores and cross sections to a fine polish, progressively from ANSI 80-grit to 400-grit sandpaper, to ensure visibility of tree-ring boundaries. We then measured total ring width to the nearest 0.001 mm using scanned images and the software WinDENDRO (Regents, Inc. ver. 2012a). To measure extremely narrow or resinous rings, we used a Velmex measuring system coupled with Measure J2X (VoorTech, ver. 5.0) software. When rings were too small and in some cases obscured by resin to measure, or when rings did not crossdate, we used ring counts to estimate inner (n=3) and outer (n=5) ring dates.

We performed segmented, time-series correlation analyses in the software COFECHA (Holmes, 1983) to first relatively date and then absolutely date the tree rings on remnant samples.

COFECHA provides an output containing potential relative dating adjustments with correlations and associated *t*-values. We used a standard *t*-value of ⩾3.5, along with a minimum interseries correlation coefficient of ⩾0.40 to indicate statistical crossdating between different series (Holmes, 1983) and developed a set of measurement series that were dated relatively to each other, but had not yet been anchored in time. We then used the same analyses in COFECHA to absolutely date the floating FTL chronologies against reference chronologies for whitebark pine (Mount Washburn, WY050, 44.798 °N 110.434 °W, 937–1998 CE) (King, 2014) and Engelmann spruce (Sylvan Pass, WY023, 44.464 °N 110.131 °W, 1388–1983 CE) (Briffa and Schweingruber, 2002), both approximately 70 km from FTL, downloaded from the International Tree-Ring Data Bank (ITRDB, 2019). Early in the process, the temporal depths of the living whitebark pine and Engelmann spruce chronologies were not sufficient for use as reference chronologies for the remnant samples. Once sufficient temporal depth was achieved, we also used the living chronologies from FTL for the absolute dating of remnant samples. We tested the remaining remnant series one at a time against the growing data set and added a series to the chronology when its interseries correlation coefficient was ⩾0.40 and COFECHA suggested no statistically significant secondary temporal adjustments.

To quality-check absolute dating, evaluate chronology statistics, and develop final whitebark pine and Engelmann spruce tree-ring chronologies for FTL, we again performed segmented, time-series correlation analyses using COFECHA (Holmes, 1983). We evaluated 50-year segments, lagged by 25 years, and used an interseries correlation cutoff of ⩾0.40 to consider a tree-ring series as crossdated with the other series. We evaluated the strength of the common signal in these chronologies using the interseries correlation statistics in COFECHA and the expressed population signal (EPS) (Wigley et al., 1984), calculated using functions in the R dendrochronology program library (dplR) (Bunn, 2008). For further analyses, we truncated chronologies where the EPS fell below 0.85 (Wigley et al., 1984). We used a two-thirds, or 67% smoothing spline (Cook and Peters, 1981) in dplR to develop final, standardized chronologies for each species. This age-dependent detrending technique best accounted for age- and disturbance-related growth trends and changes in sample depth back in time; maintained low-frequency, and assumed climate-related trends in the tree-ring data; and did not artificially inflate the ends of our time series. For the purposes of this study, the chosen detrending technique allowed for visual examination of low-frequency growth trends at FTL. For the evaluation of additional lines of tree-ring evidence, we determined detrending techniques best suited to the analyses performed, as explained below.

Living and remnant tree establishment and mortality

We estimated establishment dates for living trees using pith estimators when no pith (tree center) was present (Applequist, 1958). We only determined establishment dates for remnant trees when pith was present. We report establishment dates in decadal, 10-year bins to reasonably accommodate error in these estimates and based on age-correction statistics from a previous study at the site (Axelson et al., 2014). To evaluate remnant tree mortality, we recorded if remnant trees still possessed: (1) sapwood, (2) curvature, or (3) bark. Curvature was indicated by a smooth, outer surface along a continuous ring boundary and in conjunction with sapwood. Sapwood was indicated by color and the presence of beetle galleries. These characteristics indicate death dates (curvature and/or bark) or dates near the time of death (sapwood). Remnant trees with remaining curvature had sapwood and a smooth outer surface that followed a ring boundary for all or a portion of remnant circumference. We used 50-year bins for mortality estimates to account for potential error and based on estimated rings per cm calculated from intact sapwood on living and remnant trees.

Analyses of tree growth patterns

To evaluate potential correspondence between changes in tree growth and periods of climate change, establishment, or mortality, we identified single years of substantial negative growth change and periods of growth suppression. First, we determined ring-width minima (narrowest 5% of ring-width indices) and multi-year periods of reduced growth (at least three minimum years within a decade) within standardized FTL chronologies. To emphasize both the most negative growth years and periods of decreased growth within a decade, we standardized raw tree-ring data using a highly flexible 32-year spline. We then compared ring-width minima with pointer years and periods of growth suppression detected by relative growth change analyses (15-year moving window) in the R package PointRes (Van der Maaten-Theunissen et al., 2015). We used the raw ring-width chronologies for these analyses, and set the following thresholds for pointer years in R: (1) Growth Suppression: 40% relative growth change, and (2) Minimum Percent Recording Trees: 75%, according to Schweingruber et al. (1990) and the defaults used in pointRes (Van der Maaten-Theunissen et al., 2015), such that a pointer year marking extreme negative growth change would be a year where >75% of recording trees experienced a >40% reduction in growth. We compared growth reductions to establishment, mortality, and frost ring data from FTL tree rings and to blue-intensity based, reconstructed summer temperature values for the FTL site.

Blue intensity data

We evaluated blue intensity (BI, McCarroll et al., 2002) data, an innovative approach in dendroclimatology and alternative to maximum latewood density, for reconstructing temperature (Björklund et al., 2015; Heeter et al., 2019, 2020; Wilson et al., 2014) from FTL Engelmann spruce tree rings. To develop BI series, we refinished the Engelmann spruce samples up to 1000 grit and rescanned them on an Epson 12000 XL flatbed scanner at 3200 dpi, calibrated using an IT8.7.2 calibration card coupled with Silverfast 7.9 software. As the quality and consistency of BI measurements rely heavily on the appearance and color of sample surfaces, we developed our BI chronologies from samples that did not exhibit discoloration from weathering or fungal staining. We measured earlywood (EWB), latewood (LWB), and delta (ΔB) BI from scanned samples using the software CooRecorder (Larsson, 2014) and ultimately obtained BI metrics from 86 samples. We checked BI data crossdating using COFECHA (Holmes, 1983), detrended the data using an age-dependent spline in the SignalFree framework (Melvin and Briffa, 2008), and evaluated signal strength using the EPS statistic, with cutoff of 0.85 (Wigley et al., 1984).

We evaluated the climate sensitivity and reconstruction potential of BI data from Engelmann spruce and compared this to the reconstruction potential of full ring-width data from both Engelmann spruce and whitebark pine. We examined spatial relationships between ring-width and EWB, LWB, ΔB data and monthly mean, maximum, and minimum and seasonal average temperature variables derived from the nearest gridpoint to FTL in the CRU 4.3 dataset (Harris et al., 2014) in KNMI Climate Explorer (Trouet and Van Oldenborgh, 2013). We also examined spatial correlations in 1 to 5-year time steps back in time to assess the temporal stability of significant relationships over the instrumental period 1920–2016 CE. Based on these comparisons, we selected LWB data from Engelmann spruce for use in the reconstruction; LWB exhibited the strongest relationship overall:

Table 1. Final remnant, living, and combined chronologies developed by this study and associated statistics.

Chronology[1]	Measured series	Total trees	Length (yrs)	Mean length series (yrs)	Average interseries correlation	Average mean sensitivity	Percent segments flagged[2]	Time span (CE)	EPS	Rbar
Remnant PIAL	134	78	1250	340.7	0.54	0.22	9.97	708–1958	0.94	0.30
Remnant PIEN	44	28	1253	341.4	0.63	0.22	3.70	754–2007	0.83	0.29
Living PIAL	299	148	684	136.0	0.60	0.24	9.87	1332–2016	0.96	0.28
Living PIEN	232	118	364	148.0	0.63	0.23	8.86	1652–2016	0.97	0.27
Combined PIAL	433	226	1308	199.0	0.57	0.23	7.69	708–2016	0.96	0.29
Combined PIEN	276	146	1262	178.0	0.63	0.23	3.61	754–2016	0.94	0.28
PIEN LWB	86	58	417	172.1	0.54	0.042	18.58	1600–2016	0.92	0.33

[1] ITRDB Species Codes, where PIAL = whitebark pine (Pinus albicaulis Engelm.) and PIEN = Engelmann spruce (Picea engelmannii Parry ex Engelm.)
[2] Indicates percent of tested segments in COFECHA for which the interseries correlation fell below the statistical threshold for significance at the 0.01 level. These were re-inspected and found to be correctly placed in time.

$r=0.63$ with the average of June, July, and August (JJA) maximum temperatures ($T_{\max}$), as compared to the strongest relationship between Engelmann spruce ring widths and JJA $T_{\max}$: $r=0.40$. This finding is consistent with previous studies that demonstrate the strength of BI-temperature relationships over ring-width data (Harley et al., 2021; Heeter et al., 2019, 2020; Wilson et al., 2014).

Temperature reconstruction

We used linear regression to model JJA $T_{\max}$ back to 1600 CE using a combination of regional instrumental data and the FTL LWB chronology. We used cross-validation (Meko, 1997; Michaelsen, 1987) to validate the reconstruction model, splitting the instrumental period into two equal halves, early (1920–1960 CE) and late (1961–2015 CE), with the earliest year (1920 CE) representing when at least two stations were available for interpolation into the CRU dataset for FTL. We first calibrated on the late period and verified on the early period, and then calibrated on the early and verified on the late period to ensure the time stability of the model. We used two goodness-of-fit statistics, the reduction of error (RE) and coefficient of efficiency (CE), in which positive values indicate that the model is a better predictor than the average of the instrumental data over the same period (Cook et al., 1999; Fritts, 2001). Final cross-validation statistics included calibration and verification period coefficient of determination (CR^2 and VR^2), verification period RE and CE (VRE and VCE), and root mean squared error (RMSE). With successful model validation, we used linear regression to reconstruct the chosen temperature variable. We used the Durbin-Watson statistic to evaluate the model residuals for first-order autocorrelation and linear trends (Durbin and Watson, 1971) and quantified model uncertainty using maximum entropy bootstrapping (MEBoot), set at 300 replicates (Vinod and López-de-Lacalle, 2009). We transformed reconstructed values to *z*-scores, using the mean and standard deviation calculated over the full reconstructed record to examine annual and 10 and 20-year temperature anomalies. We used runs analysis, also known as severity-duration analysis (Bekker et al., 2014; González and Valdés, 2003; Gray et al., 2011; Griffin and Anchukaitis, 2014), performed on the non-standardized reconstructed temperature values to determine the magnitude and intensity of temperature changes.

Results

Living tree establishment

The final living whitebark pine chronology covered the period 1332–2016 CE, and the final living Engelmann spruce chronology covered the period 1652–2016 CE (Table 1). We estimated establishment dates for 84% of the crossdated, living trees (for 124 of 128 whitebark pine trees and 99 of 118 Engelmann spruce trees). The establishment dates for both species indicate an increase in establishment after the end of the LIA; most whitebark pine (>76%) and Engelmann spruce (>65%) established after 1850 CE (Figure 2c and e). The remaining trees established during earlier portions of the LIA (pre-1715 CE), except for one whitebark pine tree that established during the MCA (~1282 CE) and survived until the present. An additional whitebark pine tree had an inner measured ring indicating establishment during the MCA (1332 CE), but we could not determine an exact establishment date due to irregular growth near the innermost rings. These two living whitebark pine predate the establishment of the next oldest whitebark pine (1506 CE) by about two centuries and the next oldest Engelmann spruce (1621 CE) by about three centuries.

Remnant tree establishment and mortality

We initially developed site-specific reference chronologies for each tree species through successful crossdating with statistical significance of 15 whitebark pine remnants against the Mount Washburn reference chronology ($r=0.45$, $n=874$ years, $t=14.88$, $p<0.0001$) and 15 Engelmann spruce remnants against the Sylvan Pass reference chronology ($r=0.43$, $n=596$ years, $t=11.61$, $p<0.0001$). We then dated an additional 76 remnant trees against the GYE and FTL living reference chronologies for a total of 106 dated remnants from the FTL site (Figure 3, Supplemental Table S1). Of the 78 whitebark pine remnants sampled, 37 (47%) contained evidence of preserved outer rings (Supplemental Table S1). Excluding those trees without definitive inner- and outer-ring dates, 12 of 21 (57%) whitebark pine remnants indicated establishment before or during the MCA and mortality during the period 1593–1807 CE, or the middle-to-late LIA. An additional seven of the 21 (33%) established during the period 1379–1498 CE (early-to-middle LIA) and died during the period 1757–1832 CE (middle-to-late LIA). Of 16 whitebark pine remnants without pith but possessing intact outer rings, two had terminal ring dates during the early-to-middle LIA and 10 had terminal-ring dates during the middle-to-late LIA. In total, 31 of the 37 (84%) whitebark pine remnants with evidence of outer rings indicated terminal dates during the LIA, and more specifically, 29 of the 37 (78%) had terminal ring dates during the middle-to-late LIA (Figure 3, Supplemental Table S1). Of the 28 Engelmann spruce remnants sampled, 19 (68%) contained evidence of preserved outer rings (Supplemental Table S1). Excluding those trees without definitive inner- and outer-ring dates, four of 11 (36%) Engelmann spruce remnants indicated establishment during the MCA and mortality during the period 1608–1800 CE, or the middle-to-late LIA. An additional three of the 11 (27%) established during the period 1527–1576 (early-to-middle LIA) and died during the period 1800–1876 CE (middle-to-LIA). All of the Engelmann spruce remnants without pith but possessing intact outer rings (eight of eight) had terminal-ring dates during the middle-to-late LIA. All 15 of the 19 (79%) Engelmann spruce remnants with evidence of outer rings indicated

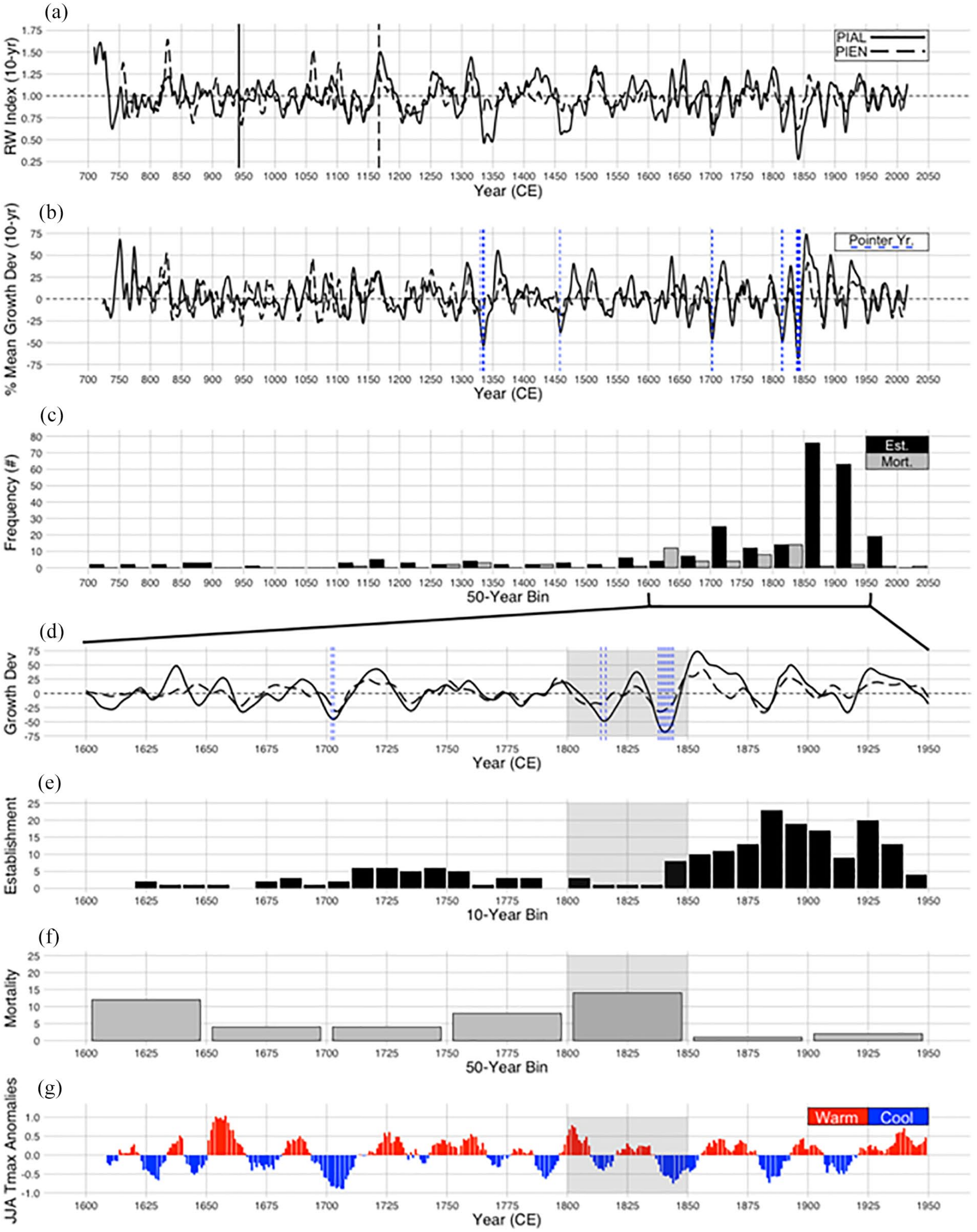

Figure 2. Comparisons of (a) Full-length, 10-yr smoothed ring-width index series for whitebark pine (PIAL) and Engelmann spruce (PIEN) where vertical dashed lines indicate EPS cutoff year (EPS < 0.85), (b) 10-yr smoothed, mean growth deviation from relative growth change analyses, with pointer years indicated by vertical, dashed blue lines, (c) Establishment and mortality frequency (# of trees) per 50-year bin over the full ring-width record, and for the period 1600–1950 CE: (d) mean growth deviation and pointer years, (e) establishment frequency in decadal bins, (f) mortality frequency in 50-year bins, and (g) 10-yr reconstructed JJA T_{max} anomalies (z-scores). Grey area highlights the late LIA period 1800–1850 CE.

terminal dates during the middle-to-late LIA (Figure 3, Supplemental Table S1). For both species combined, 46 of 56 (82%) total remnant samples with preserved outer rings had terminal-ring dates during the LIA, and more specifically, 44 of 56 (78%) had terminal ring dates during the middle-to-late LIA (Figures 2c, f and 3). Remnant spruce trees with intact pith and sapwood (n=11) were on average 375 years old when they died, and remnant spruce trees without pith but with some sapwood (n=8) contained on average 437 rings. Remnant whitebark pine trees with intact pith and sapwood (n=21) were on average 446 years old when they died, and remnant whitebark pine trees without pith but with some sapwood (n=16) contained on average 397 rings. The average age of all

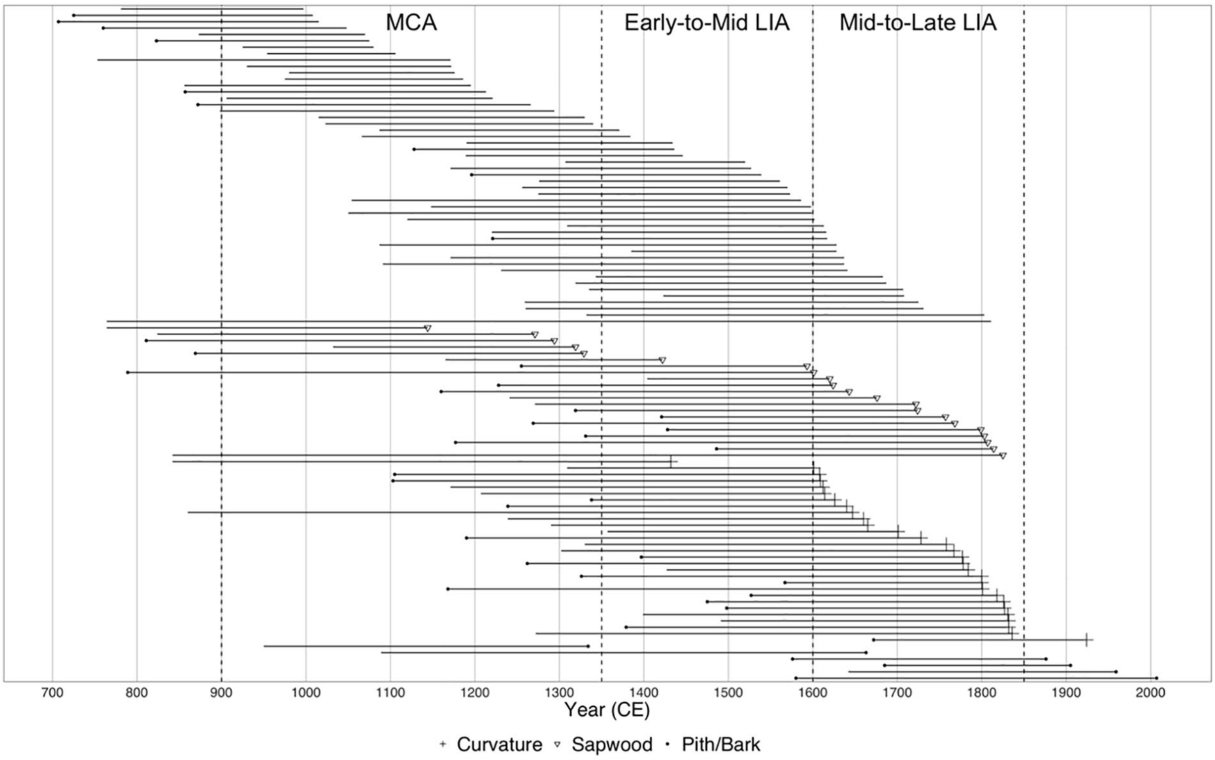

Figure 3. Plot of series time spans, which shows inner and outermost rings (and ring types) in relation to the MCA and early-to-middle and middle-to-late LIA. Note that despite establishment, few trees survived the extent of the LIA.

remnant trees with intact pith and sapwood ($n=32$) was 422 years, and remnant samples without pith but with some sapwood ($n=24$) contained on average 411 rings, for an average of 417 years ($n=56$, SD=126).

Final chronologies and analyses of growth

The final whitebark pine chronology covered the period 708–2016 CE, and the final Engelmann spruce chronology covered the period 754–2016 CE (Figure 2a, Table 1). Multiple periods of suppressed growth are evident in both FTL tree-ring chronologies for the last millennium, especially for whitebark pine (Figure 2a and b, Table 2). Based on tree-ring minima and relative growth change analyses, notable periods of decreased growth include the 1330s, 1450s, early 1700s, 1810s, and 1830/40s (Figure 2b, Table 2). Decreased growth during the 1330s was the most extreme growth suppression detected by our analyses, aside from the narrow rings and growth suppressions of the 19th century. The years 1330 and 1335 CE are two of the five most extreme tree-ring minima in FTL whitebark pine, and 1330 CE is the tenth most extreme tree-ring minimum in FTL Engelmann spruce. Relative growth change analyses also revealed narrow rings and suppression in whitebark pine during the 1330s CE, with pointer years 1330 and 1334–1336 CE (Figure 2b). We identified only one frost ring in 1329 CE associated with this period of suppressed growth (Table 2). For the 1450s, only 1 year, 1458 CE, is indicated by both relative growth change analyses and tree-ring minima, and only in whitebark pine (fourth most narrow ring) (Figure 2b, Table 2). Decreased growth in the period 1700–1710 CE is indicated by pointer years in whitebark pine (1702–1703) and tree-ring minima in both tree species (1702–1704 and 1704–1707 respectively) (Figure 2b and d, Table 2). Decreased growth during the 1450s and early 1700s was not associated with any frost damage in tree rings (Table 2).

Growth suppressions during the 1810s and 1830/40s CE are most extreme in the FTL whitebark pine chronology. Thirteen of the narrowest 5% ($n=59$) of tree-ring minima for whitebark pine occur during the periods 1814–1818 CE ($n=5$) and 1838–1845 CE ($n=8$) (Table 2). In addition, six of the narrowest 1% ($n=12$) of tree-ring minima for whitebark pine occur in the period 1838–1844 CE. Relative growth change analyses of raw ring widths in whitebark pine trees also revealed pointer years in 1814 and 1816 CE and every year from 1838–1844 CE (Figure 2b and d). In FTL Engelmann spruce, ring-width indices for the years 1814, 1838, 1844, and 1845 CE fall within the narrowest 5% ($n=43$) of ring-width minima (Table 2). The year 1838 CE was the only pointer year identified by relative growth change analysis in PointRes for Engelmann spruce tree rings at FTL. The 1838 CE growth ring was the most extreme tree-ring minimum in the whitebark pine chronology and the second most extreme in the Engelmann spruce chronology. In addition to decreased growth, we identified a cluster of latewood frost rings in the 1830s (1832, 1836, 1837, and 1838 CE) (Table 2). Frost rings (Figure S1) occur when temperatures well below freezing occur during the growing season, which can lead to intracellular freezing and the deformation of cell structure. While frost rings are not uncommon in FTL tree rings (Table 2), the 1830s is the only period in which a sequence of frost rings occurred in conjunction with prolonged suppressed growth. In all, the most extreme periods of decreased growth occurred during the periods 1330–1336 and 1838–1844 CE in whitebark pine.

Blue intensity-based temperature reconstruction

We developed a reconstruction of summer (JJA) T_{max} back to 1600 CE using a combination of regional instrumental data and the FTL LWB chronology (Figure 4, Table 1). Examination of multiple datasets of temperature variables indicated that the LWB chronology exhibited the strongest, positive, and significant ($r=0.63$, $p<0.01$) relationship with JJA T_{max} (°C) derived from the CRU 4.3 dataset (Harris et al., 2014). This relationship was temporally stable over the period 1920–2016 CE. We determined that the LWB chronology had adequate sample depth for a reconstruction over the period 1600–2016 CE. Cross-validation statistics (Table 3) indicated robust predictive skill over the instrumental period (Figure 4a and b). The reconstructed JJA T_{max} record (Figure 4c and d) displays decadal to multi-decadal variability in summer temperatures over the last four

Table 2. Tree-ring minima (narrowest 5%) from the FTL whitebark pine and Engelmann spruce chronologies.

Century (CE)	Year(s)
FTL Whitebark Pine	
9th	847 (898)
10th	946, 990 (945, 981, 993, 996)
11th	1009 (1008, 1049, 1066)
12th	1118, 1120, 1142
13th	1200, 1230 (1274)
14th	1330, 1334, 1335, 1336, 1351 (1329)
15th	1408, 1458, 1475 (1472)
16th	1541 (1537,1557)
17th	1612, 1618, 1627, 1646, 1647, 1663, 1664, 1667, 1680, 1681 (1601, 1641)
18th	1702, 1703, 1704, 1755, 1779, 1782, 1791 (1725)
19th	1814, 1815, 1816, 1817, 1818, 1838, 1839, 1840, 1841, 1842, 1843, 1844, 1845, 1883, 1884, 1899 (1832, 1836, 1837, 1838)
20th	1915, 1916, 1917, 1918, 1951, 1966, 1989, 1996 (1965)
21st	—
FTL Engelmann Spruce	
9th	—
10th	—
11th	—
12th	1192
13th	1204, 1223, 1226, 1244
14th	1321, 1330, 1366, 1383, 1393, 1399
15th	1408, 1417, 1429, 1447
16th	1500, 1505, 1524, 1596
17th	1601, 1641, 1663
18th	1704, 1705, 1706, 1707, 1746, 1791
19th	1809, 1814, 1838, 1844, 1845, 1879, 1883, 1884
20th	1971, 1972, 1989, 1992, 1993
21st	2004, 2007

Frost rings for each century are noted in parentheses for whitebark pine and did not occur in Engelmann spruce.

centuries, thereby capturing both warmer and cooler periods within the middle-to-late LIA. The coolest periods of the full reconstructed record center on 1699, 1841, and 1971 CE (Figure 4d, Table 4); the coolest, 20-year periods, not reported in Table 4 are: 1962–1981, 1690–1709, and 1832–1851 CE, with average z-scores of −0.80, −0.56, and −0.50, respectively. These periods were also ranked by severity-duration analysis within the top-10 of 88 total cooling events captured in the reconstruction from 1600–1950 CE (Table 4). They mark the two coolest periods of the middle-to-late LIA and a 20th century cool event lasting nearly four decades (1960–2000 CE) (Figure 4d). The warmest periods of the full reconstructed record center on 1654 and 2006 CE (Figure 4d, Table 4); the warmest, 20-year periods, not reported in Table 4, are 1645–1664 and 1997–2016 CE, which have average z-scores of 0.66 and 0.64, respectively. These periods are ranked by severity-duration analysis within the top-10 of 89 warm events captured by the reconstruction (Table 4). They mark both the warmest period of the middle-to-late LIA, and modern warming, marked by short duration but high magnitude (highest intensity) warming events in 2011–2013 and 2015–2016 (Table 4).

Discussion

Climate-induced mortality

Analysis of remnant and living trees at FTL provided a basis to evaluate the influence of past climate on growth and establishment in high-elevation whitebark pine and Engelmann spruce. Tree-ring dating of remnant samples suggests that the large dead trees at FTL represent the remains of an open woodland that established and grew during the late MCA (1100–1350 CE) and perished during the middle-to-late LIA (1600–1850 CE). Temporal patterns of establishment and mortality, along with tree growth patterns and frost damage, indicate conditions favorable to recruitment during the latter half of the MCA and possible climate-induced mortality of trees during the middle-to-late LIA. This period of higher mortality was followed by a period of low recruitment and rare survival during the first half of the 19th century. While mortality dates were spread throughout the LIA, few of the remnant trees survived past the end of the LIA at 1850 CE, and more than 65% of living trees established after this date. While some trees did establish and survive through the LIA, results indicate that conditions during the middle-to-late LIA were primarily unfavorable to seedlings as well as mature trees. The near eradication of trees from the FTL site during the middle-to-late LIA points to drastically different environmental conditions at this time than during the preceding MCA, when many of the large trees established, and indicates a climate event significant enough to kill a mature, ancient forest that is unparalleled in the contemporary period. The removal of most mature, old whitebark pine and Engelmann spruce (~422 years, ~70–90 cm diameter) and their replacement by younger trees (~142 years, ~38.6 cm diameter) after 1850 CE indicates that the site was potentially affected by shifting treeline during the middle-to-late LIA. The few trees that survived the middle-to-late LIA likely occupied more favorable microclimates within the complex site topography or benefitted from facilitation. These factors are important local drivers of treeline migration, and of conifer establishment and survival at high elevations (Bekker, 2005; Elliott, 2011; Elsen and Tingley, 2015; Holtmeier and Broll, 2005; Pyatt et al., 2016; Resler et al., 2005).

Although fire or insect disturbance could have killed trees at the FTL site, the asynchronous patterns of mortality point to climate change as the most likely driver of tree mortality. We found only limited evidence of fires and insect outbreaks in our samples. The spatial distribution of the handful of cross-sections on which we identified fire scars indicates that the fires were small and isolated, likely lightning-started and affecting only one to a few trees. While cooler and wetter conditions during the LIA led to increased fuels and fire in ponderosa pine (*Pinus ponderosa* Douglas ex P. Lawson & C. Lawson) ecosystems of the GYE, these fires were found to be low severity and not stand replacing (Pierce et al., 2004). We found little to no evidence of the blue stain fungi *Ceratocystis montia* Rumb. or *Europhium clavigerum* Robinson and Davidson in the sapwood of remnant trees, markers for bark beetles (Reid et al., 1967; Solheim, 1995; Whitney, 1971). We also rule out old age as the cause of mortality based on the average age of remnants containing intact pith and outer rings (422 years); while advanced, this is less than the maximum identified ages for whitebark pine and Engelmann spruce (>600 years, this study, Fryer, 2002; Luckman et al., 1984; Perkins and Swetnam, 1996; Steele et al., 1983; USDA, 2013).

We interpret tree death during the LIA as driven by climate, based on (1) asynchronous but tightly clustered patterns of mortality, (2) the lack of widespread evidence of fire- or insect-induced mortality at FTL, (3) the fact that growing season temperatures are most limiting to growth in high-elevation trees (Fritts, 2001; Rossi et al., 2008), and (4) the importance of growing-season length to ring formation in whitebark pine, such that a ring may not form if growing-season length falls below 3 months, most often due to cold temperatures (Weaver, 2001). Based on these lines of evidence, we interpret the current landscape at FTL as representative of post-1850 recovery from late LIA treeline decline and the transition into late-20th century, anthropogenic warming. We further suggest climate-induced mortality as the dominant driver of treeline change at FTL based on additional lines of tree-ring evidence, which highlight the final phase of the

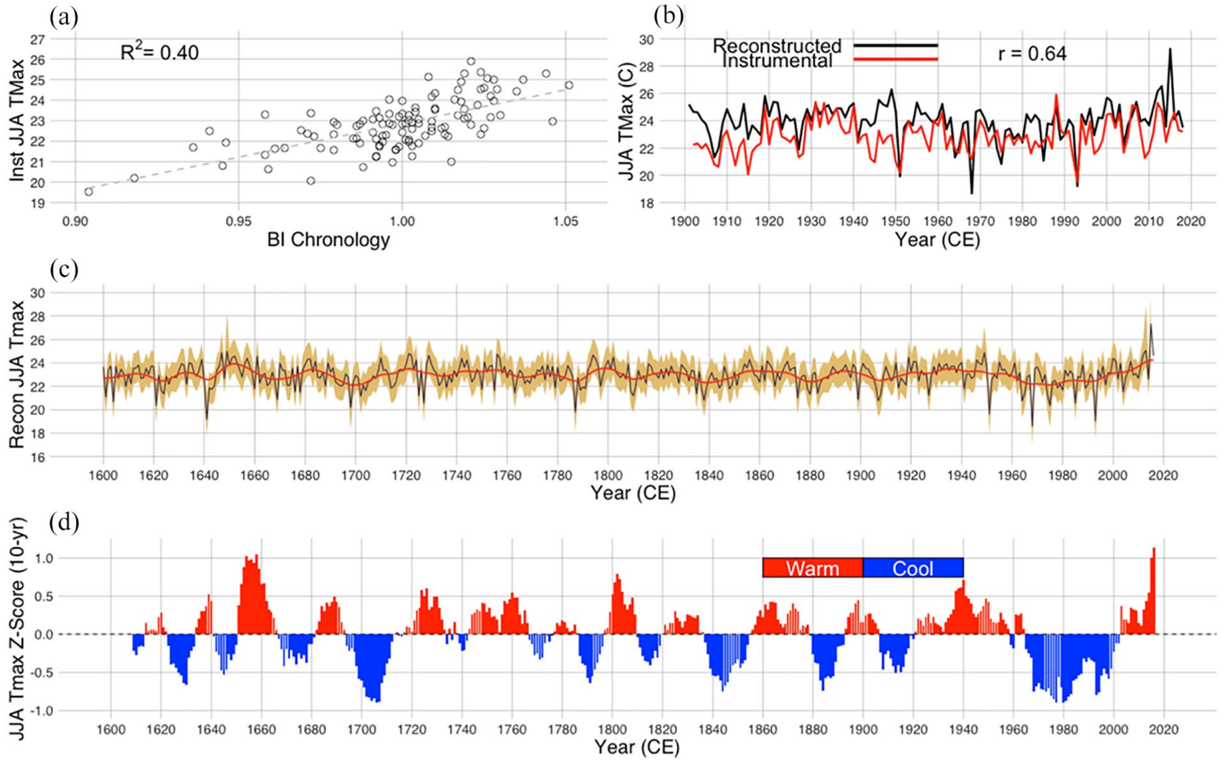

Figure 4. Summer (JJA) T_{max} (°C) reconstruction for FTL: (a) Scatter plot of the CRU 4.3 instrumental JJA T_{max} values versus LWB with linear function $y = -1.173 + 24.003\times$ (dashed), (b) Comparison of CRU 4.3 instrumental (red) and reconstructed (black) JJA T_{max} values, (c) Reconstruction of JJA T_{max} using FTL LWB chronology from 1600–2016 CE, smoothed with 20-year low-pass filter (red), and (d) 10-year running average of reconstructed JJA T_{max} anomalies (z-scores), calculated using the mean and standard deviation of 1600–2016 CE reconstructed values.

Table 3. Cross-validation statistics for the final reconstruction model $y = -1.173 + 24.003x$.

Calibration period	Verification period	CR^2	VR^2	VRE	VCE	RMSE
1961–2015	1920–1960	0.45	0.33	0.33	0.31	0.92
1920–1960	1961–2015	0.33	0.45	0.40	0.38	0.98

LIA as one of the coldest periods over the last four centuries, and potentially over the last millennium in the GYE. We discuss these multiple lines of evidence in the following sections, focusing our interpretation of the correspondence between climate, establishment, and mortality to the period 1600–1950 CE (Figure 2d–g). The focus on this period is due to lower sample depths for establishment and mortality data prior to 1600 CE, the skillful length of the reconstruction, and the fact that our study design did not include saplings.

The terminus of the LIA

The middle-to-late LIA (1600–1850 CE) was a period of increased mortality and decreased recruitment of trees, with a majority of current, mature trees at FTL having established after 1850 CE. Growth patterns of both species, and especially whitebark pine, track reconstructed summer temperatures well (Figure 2d and g). This highlights the importance of temperatures to tree growth during short growing seasons, approximately 3 months, at high elevation sites like FTL. Within the middle-to-late LIA, periods of higher mortality and reduced establishment correspond with generally cooler periods, broken only by short and/or weak (low summer maximum temperatures) periods of warmth, for example, approximately 1600–1650, 1770–1800, and 1810–1855 CE (Figure 2e–g). This is especially evident in the 1810–1855 CE period; limited temperature recovery after cooling during the 1810s does not appear to have been sufficient to support recruitment of either tree species before the return to cold conditions in the late 1830s. Apart from a few years of warmth during the turn of the 19th century, cooler conditions persisted for nearly 100 years, from approximately 1770–1855 CE, likely resulting in low recruitment and high mortality. In contrast, increased establishment during 1710–1760 CE (Figure 2e) occurred during a period of prolonged relative warmth, interrupted only by short and/or weak cooling. Within the middle-to-late LIA, periods of increased mortality and decreased recruitment correspond with longer periods consisting of multiple, decade-long episodes of cooler summers (much of the middle-to-late LIA), with one period of increased establishment and decreased mortality (1710–1760 CE) having occurred during a longer period of relative warmth. These patterns, however, do not hold for periods after 1850 CE, with increased establishment and decreased mortality during two cold periods, 1875–1884 and 1904–1913 CE, suggesting different influences on more recent patterns of growth, establishment, and mortality.

Comparisons to local summer (average of June, July, August, JJA) Palmer Drought Severity Index (PDSI) (Cook et al., 2010) and April 1st snow-water equivalent (SWE) (Coulthard et al., 2019) reconstructions for the GYE (Figure 5) reveal the potential compounding influence of snowpack or drought at FTL, although patterns are less clear than for temperature. In our comparison, summertime PDSI represents soil moisture conditions with high, positive values indicating wetter conditions and low, negative values indicating drier conditions (Cook et al., 1999; Palmer, 1965), and April 1st SWE reflects the maximum annual snowpack measurement in the region (Coulthard et al., 2019) (Figure 5). Within 1600–1950 CE, periods of reduced growth, decreased establishment, and increased mortality are consistently associated with cooler summer temperatures but less consistently with drought or snowpack. The

Table 4. (Left) Anomalies (z-scores) are calculated over the full reconstructed period (1600–2016 CE) and (Right) Results from runs analysis based on FTL reconstructed JJA T_{max} (°C) values. Magnitude equals the mean cumulative departure from the mean of reconstructed values. Intensity equals duration (years) divided by the magnitude. After ranking, overall score equals duration plus magnitude rank.

Single and 10-year anomalies						Runs analysis						
Coldest rank	Year (CE)	JJA T_{max} (°C)	*Z*-score	10-year anomaly	Avg. *Z*-Score	Period	Duration (years)	Magnitude	Intensity	Duration rank	Magnitude rank	Overall score
1	1968	18.59	−4.39	1697–1706	−0.90	1697–1708	12	−9.34	−0.78	9	88	97
2	1993	19.03	−3.95	1971–1980	−0.90	1974–1980	7	−8.49	−1.21	7	87	94
3	1641	19.18	−3.79	1984–1993	−0.80	1964–1968	5	−8.31	−1.66	5	86	91
4	1951	19.62	−3.36	1959–1968	−0.76	1621–1629	9	−7.05	−0.78	8	83	91
5	1787	19.82	−3.16	1835–1844	−0.76	1640–1644	5	−7.45	−1.49	5	85	90
6	1698	20.21	−2.76	1875–1884	−0.74	1786–1791	6	−7.08	−1.18	6	84	90
7	1621	20.37	−2.60	1621–1630	−0.67	1875–1880	6	−5.38	−0.90	6	82	88
8	1975	20.37	−2.60	1782–1791	−0.64	1905–1909	5	−5.12	−1.02	5	81	86
9	1727	20.57	−2.41	1636–1645	−0.54	1837–1840	4	−4.61	−1.15	4	80	84
10	1985	20.57	−2.41	1904–1913	−0.51	1992–1993	2	−4.24	−2.12	2	79	81
Warmest rank	Year (CE)	JJA T_{max} (°C)	*Z*-score	10-year anomaly	Avg. *Z*–score	Period	Duration (years)	Magnitude	Intensity	Duration rank	Magnitude rank	Overall score
1	2015	27.31	4.37	2007–2016	1.13	1929–1940	12	7.90	0.66	8	89	97
2	2013	25.07	2.11	1649–1658	1.04	1717–1724	8	7.39	0.92	7	87	94
3	1649	24.99	2.03	1793–1802	0.79	1649–1654	6	7.48	1.25	6	88	94
4	1647	24.87	1.91	1931–1940	0.72	1679–1684	6	5.39	0.90	6	84	90
5	1949	24.87	1.91	1717–1726	0.60	1946–1950	5	5.66	1.13	5	85	90
6	1721	24.79	1.83	1751–1760	0.55	1792–1796	5	5.22	1.04	5	83	88
7	1756	24.75	1.79	1630–1639	0.52	2015–2016	2	5.99	2.99	2	86	88
8	2012	24.75	1.79	1680–1689	0.50	1798–1803	6	4.37	0.73	6	81	87
9	1722	24.67	1.71	1940–1949	0.47	1741–1745	5	4.28	0.86	5	80	85
10	1794	24.67	1.71	1889–1898	0.45	2011–2013	3	4.69	1.56	3	82	85

periods 1697–1706 and 1814–1818 CE were cold, dry, and snowy while 1835–1844 CE was cold, wet, and less snowy (Figure 5). Periods of increased growth, increased establishment, and decreased mortality are consistently associated with warm and dry summers but less consistently with snowpack. The periods 1717–1726 and 1889–1898 CE were warm, dry, and less snowy while 1858–1874 CE was warm, dry, and more snowy (Figure 5). Overall, warm and dry summers appear to have been most optimal for both growth and establishment at FTL, especially after 1850 CE, with pluvials, such as during the 1910s/20s, having led to slight reductions in both (Figure 5). Higher mortality overall from 1600–1850 CE is likely due to increased April 1st SWE (Coulthard et al., 2019) during much of this period, which may have limited establishment and increased mortality by limiting growing season length, especially in years with cooler summers. Negative relationships between tree growth and winter snowpack (December-January precipitation) for both studied species (Rochner, 2019) indicate the role of snowpack in limiting growing season length, and perhaps also damaging trees at FTL, rather than providing additional summer moisture or offsetting drought conditions at the site (Coulthard et al., 2021). During the terminus of the LIA, however, we see a climate shift from cold, dry, and snowy to cold, wet, and less snowy, making less clear the roles of drought and snow in treeline mortality during this period (Figure 5). Potentially, overall cold and wet conditions from 1800–1825 CE due to snow and from 1825–1850 CE due to summertime moisture made the entire period too cold and wet for establishment, while limited growing seasons and late-season frost killed mature trees.

The two coldest periods of the middle-to-late LIA were 1690–1709 and 1832–1851 CE, corresponding to the Maunder and Dalton solar minima and with volcanically-forced cool periods (Anchukaitis et al., 2017; Crowley, 2000; Crowley et al., 2008; D'Arrigo et al., 2020; Wagner and Zorita, 2005; Wilson et al., 2016) noted in other regional reconstructions in the western US and Canada (Luckman and Wilson, 2005; Salzer et al., 2014; Wilson et al., 2014). The cold and snowy Maunder Minimum especially limited establishment and led to mortality and decreased growth in both species (Figures 2e–g and 5). The period 1832–1851 CE, however, saw more transformation at FTL. Multiple lines of evidence point to the terminus of the LIA as a period of dramatic and likely climate-driven change at the site. Reconstructed cool temperature anomalies for 1800–1850 CE correspond to patterns of decreased establishment and increased mortality, decreased growth, and frost damage in whitebark pine and Engelmann spruce. The period was one of rare survival and low recruitment for both tree species (Figure 2e and f), and growth rates for surviving trees were some of the lowest of the millennial record (Figure 2a and b). These findings of exceptionally low temperatures during the late LIA are consistent with documented glacial advances in the western US and Canada (Carrara, 1989; Luckman, 2000; Marcott et al., 2009; Osborn and Gerloff, 1997; Wiles et al., 2004), and with continental and hemispheric temperature reconstructions (Anchukaitis et al., 2017; Bradley and Jonest, 1993, 1995; Briffa et al., 2001; Brönnimann et al., 2019; Crowley, 2000; Crowley et al., 2014; Jones et al., 1998; Mann et al., 2008, 2012; Trouet et al., 2013). Results from this study also agree with regional paleoclimate records that document cooler summer temperatures during the first half of the 19th century in the Canadian Rockies (Luckman and Wilson, 2005), southern British Columbia (Wilson et al., 2014), the Sawtooth-Salmon River region of Idaho (Biondi et al., 1999), the Selway-Bitterroot Wilderness Area of the northern Rocky Mountains (Kipfmueller, 2008), the US Great Basin (Salzer et al., 2014), and the southern Colorado Plateau (Salzer and Kipfmueller, 2005). The cold, final phase of the LIA has been attributed to separate solar and volcanic forcings, with eruptions in 1808, 1815, 1822, 1831, and 1835, including from Tambora and Cosigüina (Anchukaitis et al., 2017; Brönnimann et al., 2019; Crowley, 2000; Crowley et al., 2014; Hegerl et al., 2003; Wilson et al., 2016). Multiple volcanically-driven "cold snaps," especially after 1830 CE, are then the likely dominant driver of mortality at FTL.

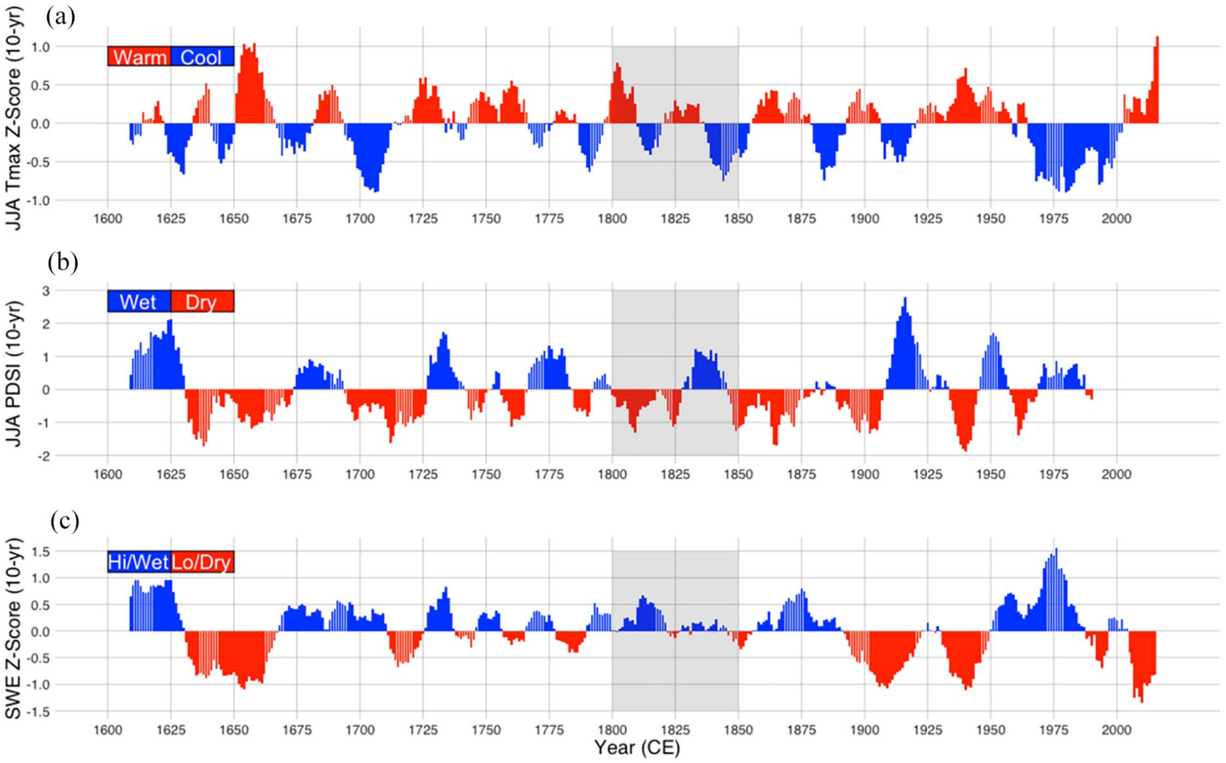

Figure 5. (a) Comparison of the JJA T_{max} anomalies from this study (10-year z-scores) with (b) reconstructed JJA PDSI (10-year) from Cook et al. (2010) and (c) reconstructed April 1st SWE (annual maximum) snowpack (10-year z-scores) from Coulthard et al. (2019) for the Greater Yellowstone. Grey area highlights the LIA terminus 1800–1850 CE.

Multiple lines of tree-ring evidence, including patterns of establishment and mortality, growth patterns, frost rings, and reconstructed summer temperatures, snowpack, and drought, indicate that the early 19th century was one of transition at FTL. Within a longer period of increased mortality and decreased establishment from 1600–1850 CE, the timing and magnitude of particular cold events at the site likely explain the heavy influence of the terminus of the LIA. The cool period 1690–1709 CE was short in duration, preceded by the warmest period of the 1600–1950 record (warmest 20-year period, 1645–1660 CE), and followed by a warm period of recovery from 1710–1760 CE (Figure 4d, Table 4). In contrast, the period 1832–1851 CE marked extreme cold at the end of nearly a century of cooling from 1770–1855 CE, broken only by a few years of warmth after 1800 CE. Growth was reduced during the early part of this period, with a slight recovery at the turn of the century, before declines in the 1810s (Figure 2d). In recent hemispheric summer temperature reconstructions, the early 19th century is marked by significant cooling, in many cases showing the coolest summer temperatures of the LIA, and marking the end of a long cooling trend throughout the LIA (Anchukaitis et al., 2017; Wilson et al., 2016). The period is marked as well by an exceptional amount of volcanic activity, expected to have driven the final cold pulse of the LIA (Anchukaitis et al., 2017; Brönnimann et al., 2019; Wilson et al., 2016). Likely, repeated effects of volcanic cooling during the LIA made the trees at FTL more vulnerable to the back-to-back, volcanically-driven cold snaps of the early 19th century, and especially to the sudden drop in temperatures after 1830 CE. This vulnerability was likely enhanced by the fact that FTL trees were at the limit of their elevational range and advanced in age (~422 years) for both species. While likely not the cause of death based on maximum ages for both species (> 600 years, Fryer, 2002; Luckman et al., 1984; Perkins and Swetnam, 1996; Rose et al., 1996; Steele et al., 1983; USDA, 2013), more advanced tree ages may have increased vulnerability to colder temperatures. Age may have also played a role in decreased mortality during earlier cold periods like the Maunder Minimum when the remnant trees were younger, as well after 1850 CE when new trees had established. The influence of the 1832–1851 CE period is marked in surviving trees by the continuous sequence of marker years and tree-ring minima (growth decline), predominately in whitebark pine, from 1838–1844 CE, as well as by latewood frost damage in the years 1832 and 1836–1838 CE. The continual decrease in growth each year indicates conditions unfavorable to growth and recruitment. Latewood frost damage during these years in particular points to abrupt ends to already short growing seasons for multiple years, highlighting the importance of the timing of cold in frost damage, and potentially mortality. Compared to the 1830s, the cold period 1690–1709 CE is not marked by frost damage in the tree-ring record (Table 2). Further research is necessary to examine the role of seasonal timing in the influence of cold on tree growth and mortality. Eventually, most of the trees that had survived earlier LIA cooling were killed by the final pulse of the LIA.

The medieval climate anomaly

Temporal patterns of establishment and mortality indicate conditions favorable to recruitment during the latter half of the MCA, but limitations in the current dataset restrict our interpretation of the MCA at FTL. Several studies from the Rocky Mountains have provided evidence of treeline fluctuations during the middle to late-Holocene, although most of these studies suggest a pre-MCA warm period, with estimated, higher elevation treelines before and sometimes declining into the MCA (Carrara and McGeehin, 2015; LaMarche, 1973; LaMarche and Mooney, 1967, 1972; Scuderi, 1987). Other studies have focused on treeline and other post-glacial changes that occurred even earlier, during warmer periods of the early to middle Holocene (Fall et al., 1995; Iglesias et al., 2015; Krause and Whitlock, 2013; Krause et al., 2015; Lynch, 1998; Mensing et al., 2012; Whitlock, 1993). Relatively little is known about how the MCA affected treeline ecosystems in the GYE. Variability in how data are presented and provided, for example, how they are standardized, from regional paleoclimate records make them difficult to compare, and many of the tree-ring based temperature reconstructions from the area do not describe conditions prior to the late MCA (Biondi et al., 1999; Kipfmueller, 2008).

We identified only one treeline study in the region that documented changes specific to the MCA, and this study indicated treeline decline, not advance, during that period (Morgan et al., 2014). At a site approximately 180 km from FTL, Morgan et al. (2014) documented treeline decline during the MCA based on radiocarbon dating of remnant trees in the Wind River Range of Wyoming. They interpreted evidence of tree death and treeline decline to reflect drought stress during the MCA, contrary to our findings at FTL that trees established during that time. While this difference may represent real disparities between FTL and the nearby Wind River Range, it may partly reflect differences in scope and methods. Radiocarbon dating can only provide ranges of potential dates, in some cases centuries-wide. In contrast, the annual resolution provided by tree-ring dating can provide exact dates. The difference in resolution of these two approaches is especially important when relating dates to short climate intervals like the MCA and LIA. Because they found remnant trees up to 100 m above modern treeline, Morgan et al. (2014) could definitively conclude that treeline was once higher at their study site. However, based on our experience at FTL, we propose that interpretations of remnant death dates would benefit from combining radiocarbon with tree-ring dating techniques, such as seen in other studies of remnant wood at treeline (Carrara and McGeehin, 2015; LaMarche, 1973). Tree-ring dating would have allowed Morgan et al. (2014) to also examine the establishment dates of remnant trees. Still, we recognize that real differences may exist between the history of treeline forests at our sites. Currently, we cannot rule out decline at FTL during the MCA; many of the remnant trees at our site established after the middle-to-late MCA, and many of those that established earlier did not survive the period (Figure 3). Extreme growth suppressions during the MCA also require further investigation (Figure 2b). The potential exists for two declines: a drought-induced decline during the early MCA, and a temperature-induced decline during the LIA, such as recorded by Lloyd and Graumlich (1997) in the southern Sierra Nevada. Warm and dry conditions are known to have caused downslope movement of whitebark pine elsewhere in the Yellowstone region during the middle Holocene (Fall et al., 1995). More data are necessary to determine if this is true for the early MCA at FTL, although it will be difficult to locate remnants of trees with intact inner and outer rings that perished during this much earlier period.

Ecosystem implications

A widespread treeline mortality event at the terminus of the LIA would have had a dramatic impact on the health and function of whitebark pine ecosystems in the GYE by killing most of the mature, old whitebark pine and Engelmann spruce on the landscape. Now, a "reset," relatively young (<150 years), and endangered whitebark pine ecosystem faces a novel future under anthropogenic climate change. Young whitebark pine and Engelmann spruce trees may thrive under warmer and drier conditions, as the previous cohort did during the middle-to-late MCA, and the landscape at FTL may eventually transition back into open woodland. Both species will likely experience initial increases in growth and recruitment under warming temperatures, such as purported during the MCA and documented during even greater warming in the GYE during the middle Holocene (Carlson et al., 2017; Fall et al., 1995; Iglesias et al., 2015; Krause and Whitlock, 2013; Krause et al., 2015; Lynch, 1998; Mensing et al., 2012; Whitlock, 1993). However, the future of FTL and similar sites in a warming world will depend on the complex interplay of climate, disturbance, and competition. Twenty-first century temperatures in the GYE have exceeded those of the last 6000 years (Shuman, 2012). Dramatic environmental and ecological changes are likely to occur with projected warming, decreased winter snowpack, and increased moisture deficits in the western US (Iglesias et al., 2015; Leung et al., 2004; Mote, 2006; Sepulveda et al., 2015; Shuman, 2012). Warmer and drier future conditions are likely to affect important competitive and facilitative relationships, including between whitebark pine and Engelmann spruce (Callaway, 1998; Hill et al., 2018; MacFarlane et al., 2013; Tomback et al., 2001, 2016; Weaver, 2001). Threats to both species, including bark beetle outbreaks, devastating wildfires, and spreading invasive species, are expected to increase under warming conditions (Bentz et al., 2010; Buermeyer et al., 2016; Hart et al., 2014; Hebertson and Jenkins, 2008; Resler and Tomback, 2008; Westerling et al., 2006, 2011). While cold, either persistent or sudden, was the most likely killer identified by this study, we do not discount the role of drought in treeline mortality. The threat of local extinction of high-elevation species in the face of warming temperatures, intensifying droughts, shifting ranges, and changes in fire regimes, forest pests, and diseases underscores the need for continued study of the ecology and history of vulnerable treeline species, to better anticipate change and to inform conservation and management.

Conclusions

The two millennial-length chronologies developed during this work provide important insight into the influence of past climate changes on GYE ecosystems. Multiple lines of dendrochronological evidence suggest climate-driven mortality of whitebark pine and Engelmann spruce trees in treeline ecosystems of the GYE during the cold, final phase of the LIA. Reconstructed negative temperature anomalies, patterns of establishment and mortality, growth suppression and decline, and frost damage in both species show 1800–1850 CE to be a period of dramatic environmental change in the region. In particular, cooler summer temperatures after 1830 CE, a period marked by the Dalton solar minimum and increased volcanic activity, strongly influenced mortality, recruitment, and the growth rates of trees at FTL. Our results provide insight into how past climate change affected important treeline species and environments of the GYE and highlight the need for more spatially-resolved climate reconstructions to better describe spatial and temporal variability in the influence of climate change during the MCA and LIA on treeline communities.

Acknowledgements

We also thank former UT graduate students Lauren Stachowiak, Kyle Landolt, and Zachary Merrill for their assistance in the field, and undergraduates Patrick Clark, Anna Fraser, Ellie Eggink, Hudson Kelley, and Jack Spining for assistance in the lab. We thank Donald J. Biddle of the University of Louisville Center for GIS for improvements to the original study site map and Laura Smith of the University of Tennessee for reviewing an earlier draft of this manuscript. We also thank the two anonymous reviewers of this manuscript for their thoughtful comments and assistance in improving the manuscript. Declarations of conflicts of interest: none.

Funding

The author(s) disclosed receipt of the following financial support for the research, authorship, and/or publication of this article: Funding for this research was provided by grants to Rochner from the Whitebark Pine Ecosystem Foundation, the American Association of Geographers (AAG), the AAG Mountain Geography Specialty Group, the AAG Biogeography Specialty

Group, the AAG Paleoenvironmental Change Specialty Group, and the Golden Key International Honour Society. Additional support was provided by the North American Dendroecological Fieldweek (NADEF), funded through National Science Foundation under grant #1759694; by NSF grant #2012482 to Harley and Heeter; and by the University of Tennessee (UT). We thank Jim Speer, Christopher Gentry, and other organizers of the 2014 NADEF, during which Rochner discovered the FTL site.

ORCID iDs

Maegen L Rochner https://orcid.org/0000-0002-2340-5428
Matthew F Bekker https://orcid.org/0000-0001-6662-3225
Sally P Horn https://orcid.org/0000-0002-0575-3664

Supplemental material

Tree-ring data will be published on the International Tree-Ring Data Bank (ITRDB) after publication of this and additional manuscripts. Core and cross section samples are archived by author M Rochner at the University of Louisville.

References

Anchukaitis KJ, Wilson R, Briffa KR et al. (2017) Last millennium Northern Hemisphere summer temperatures from tree rings: Part II, spatially resolved reconstructions. *Quaternary Science Reviews* 163: 1–22.

Applequist MB (1958) A simple pith locator for use with off-center increment cores. *Journal of Forests* 56(2): 141.

Axelson J, Coulthard B, Hart M et al. (2014) Stand dynamics of high elevation whitebark pine in Shoshone National Forest, Wyoming. Report, North American Dendroecological Fieldweek.

Bekker MF (2005) Positive feedback between tree establishment and patterns of subalpine forest advancement, Glacier National Park, Montana, USA. *Arctic, Antarctic, and Alpine Research* 37: 91–101.

Bekker MF, DeRose RJ, Buckley BM et al. (2014) A 576-year Weber River streamflow reconstruction from tree rings for water resource risk assessment in the Wasatch Front, Utah. *Journal of the American Water Resources Association* 50(5): 1338–1348.

Bentz BJ, Regniere J, Fettig CJ et al. (2010) Climate change and bark beetles of the western United States and Canada: Direct and indirect effects. *Bioscience* 60(8): 602–613.

Biondi F, Perkins DJ, Cayan DR et al. (1999) July temperature during the second millennium reconstructed from Idaho tree rings. *Geophysical Research Letters* 26(10): 1445–1448.

Björklund J, Gunnarson BE, Seftigen K et al. (2015) Using adjusted blue intensity data to attain high-quality summer temperature information: A case study from Central Scandinavia. *The Holocene* 25(3): 547–556.

Bracht BB, Stone JR and Fritz SC (2008) A diatom record of late-Holocene climate variation in the northern range of Yellowstone National Park, USA. *Quaternary International* 188(1): 149–155.

Bradley RS, Hughes MK and Diaz HF (2003) Climate in medieval time. *Science* 302(5644): 404–405.

Bradley RS and Jonest PD (1993) 'Little ice age' summer temperature variations: Their nature and relevance to recent global warming trends. *The Holocene* 3(4): 367–376.

Bradley RS and Jonest PD (eds) (1995) *Climate since AD 1500*, revis ed edn. London: Routledge.

Briffa KR and Schweingruber FH (2002) NOAA/WDS Paleoclimatology – Briffa – Sylvan Pass bei Cody – PCEN – ITRDB WY023. NOAA National Centers for Environmental Information. Available at: https://doi.org/10.25921/y3hr-2c33 (accessed 14 September 2017).

Briffa KR, Osborn TJ, Schweingruber FH et al.(2001) Low-frequency temperature variations from a northern tree ring density network. *Journal of Geophysical Research Atmospheres* 106(D3): 2929–2941.

Brönnimann S, Franke J, Nussbaumer SU et al. (2019) Last phase of the Little Ice Age forced by volcanic eruptions. *Nature Geoscience* 12(8): 650–656.

Buermeyer K, Reinhart D and Legg K (2016) Case study: Whitebark pine in the Greater Yellowstone Ecosystem. In: Hansen AJ, Monahan WB, Theobald DM et al. (eds) *Climate Change in Wildlands: Pioneering Approaches to Science and Management*. Washington, DC: Island Press, pp.304–326.

Bunn AG (2008) A dendrochronology program library in R (dplR). *Dendrochronologia* 26(2): 115–124.

Callaway RM (1998) Competition and facilitation on elevation gradients in subalpine forests of the northern Rocky Mountains. *Oikos* 82: 561–573.

Carlson KM, Coulthard B and Starzomski BM (2017) Autumn snowfall controls the annual radial growth of centenarian whitebark pine (Pinus albicaulis) in the southern Coast Mountains, British Columbia, Canada. *Arctic, Antarctic, and Alpine Research* 49(1): 101–113.

Carrara PE (1989) *Late Quaternary glacial and vegetative history of the Glacier National Park region, Montana*. U.S. Geological Survey Bulletin 1902. Denver, CO: U.S. Geological Survey, 64pp.

Carrara PE and McGeehin JP (2015) Evidence of a higher Late-Holocene treeline along the continental divide in Central Colorado. *The Holocene* 25(11): 1829–1837.

Coats S, Smerdon JE, Karnauskas KB et al. (2016) The improbable but unexceptional occurrence of megadrought clustering in the American West during the Medieval Climate Anomaly. *Environmental Research Letters* 11(7): 074025.

Cook ER, Meko DM, Stahle DW et al. (1999) Drought reconstructions for the continental United States. *Journal of Climate* 12(4): 1145–1162.

Cook ER and Peters K (1981) The smoothing spline: A new approach to standardizing forest interior tree-ring width series for dendroclimatic studies. *Tree-Ring Bulletin* 41: 45–53.

Cook ER, Seager R, Heim RR Jr et al. (2010) Megadroughts in North America: Placing IPCC projections of hydroclimatic change in a long-term paleoclimate context. *Journal of Quaternary Science* 25(1): 48–61.

Cook ER, Woodhouse CA, Eakin CM et al. (2004) Long-term aridity changes in the Western United States. *Science* 306: 1015–1018.

Coulthard BL, Anchukaitis KJ, Pederson GT et al. (2021) Snowpack signals in North American tree rings. *Environmental Research Letters* 16(3): 034037.

Coulthard BL, Pederson GT and Anchukaitis KJ (2019) The spatial footprint and frequency of historic snow droughts in Yellowstone. *Yellowstone Science* 27(1): 22–26.

Crowley TJ (2000) Causes of climate change over the past 1000 years. *Science* 289: 270–277.

Crowley TJ and Lowery TS (2000) How warm was the Medieval Warm Period? *AMBIO: A Journal of the Human Environment* 29(1): 51–54.

Crowley TJ, Obrochta SP and Liu J (2014) Recent global temperature "plateau" in the context of a new proxy reconstruction. *Earth s Future* 2(5): 281–294.

Crowley TJ, Zielinski G, Vinther B et al. (2008) Volcanism and the little ice age. *PAGES News* 16(2): 22–23.

D'Arrigo R, Klinger P, Newfield T et al. (2020) Complexity in crisis: The volcanic cold pulse of the 1690s and the consequences of Scotland's failure to cope. *Journal of Volcanology and Geothermal Research* 389: 106746.

Durbin J and Watson GS (1971) Testing for serial correlation in least squares regression. iii. *Biometrika* 58(1): 1–19.

Elliott GP (2011) Influences of 20th-century warming at the upper tree line contingent on local-scale interactions: Evidence from a latitudinal gradient in the Rocky Mountains, USA. *Global Ecology and Biogeography* 20: 46–57.

Elsen PR and Tingley MW (2015) Global mountain topography and the fate of montane species under climate change. *Nature Climate Change* 5(8): 772.

Fall PL, Davis PT and Zielinski GZ (1995) Late Quaternary vegetation and climate of the Wind River Range, Wyoming. *Quaternary Research* 43: 393–404.

Fritts HC (2001) *Tree Rings and Climate*. Caldwell, NJ: Blackburn Press.

Fryer JL (2002) Pinus albicaulis. In: *Fire Effects Information System. U.S. Department of Agriculture, Forest Service, Rocky Mountain Research Station, Fire Sciences Laboratory*. Available at: https://www.fs.fed.us/database/feis/plants/tree/pinalb/all.html (accessed 6 July 2020).

González J and Valdés JB (2003) Bivariate drought recurrence analysis using tree ring reconstructions. *Journal of Hydrologic Engineering* 8(5): 247–258.

Grace J, Berninger F and Nagy L (2002) Impacts of climate change on the tree line. *Annals of Botany* 90(4): 537–544.

Gray ST, Lukas JJ and Woodhouse CA (2011) Millennial-length records of streamflow from three major upper colorado river tributaries 1. *JAWRA Journal of the American Water Resources Association* 47(4): 702–712.

Griffin D and Anchukaitis KJ (2014) How unusual is the 2012–2014 California drought? *Geophysical Research Letters* 41(24): 9017–9023.

Harley GL, Heeter KJ, Maxwell JT et al. (2021) Towards broad-scale temperature reconstructions for Eastern North America using blue light intensity from tree rings. *International Journal of Climatology* 41: E3142–E3159.

Harris I, Jones PD, Osborn TJ et al. (2014) Updated high-resolution grids of monthly climatic observations–the CRU TS3. 10 Dataset. *International Journal of Climatology* 34(3): 623–642.

Hart SJ, Veblen TT, Eisenhart KS et al. (2014) Drought induces spruce beetle (Dendroctonus rufipennis) outbreaks across northwestern Colorado. *Ecology* 95(4): 930–939.

Hebertson EG and Jenkins MJ (2008) Climate factors associated with historic spruce beetle (Coleoptera: Curculionidae) outbreaks in Utah and Colorado. *Environmental Entomology* 37: 281–292.

Heeter KJ, Harley GL, Maxwell JT et al. (2020) Late summer temperature variability for the Southern Rocky Mountains (USA) since 1735 CE: Applying blue light intensity to low-latitude Picea engelmannii Parry ex Engelm. *Climatic Change* 1–24.

Heeter KJ, Harley GL, Van De Gevel SL et al. (2019) Blue intensity as a temperature proxy in the eastern United States: A pilot study from a southern disjunct population of Picea rubens (Sarg.). *Dendrochronologia* 55: 105–109.

Hegerl GC, Crowley TJ, Baum SK et al. (2003) Detection of volcanic, solar and greenhouse gas signals in paleo-reconstructions of Northern Hemispheric temperature. *Geophysical Research Letters* 30(5): 1242.

Herweijer C, Seager R, Cook ER et al. (2007) North American droughts of the last millennium from a gridded network of tree-ring data. *Journal of Climate* 20: 1353–1376.

Hill E, Ex S, Aldridge C et al. (2018) Overstory density, short growing seasons, and moisture limit Engelmann spruce establishment over time in high-elevation managed stands. *Canadian Journal of Forest Research* 49(1): 64–75.

Holmes RL (1983) Computer assisted quality control in tree-ring dating and measurement. *Tree-Ring Bulletin* 43: 69–78.

Holtmeier FK and Broll G (2005) Sensitivity and response of northern hemisphere altitudinal and polar treelines to environmental change at landscape and local scales. *Global Ecology and Biogeography* 14: 395–410.

Iglesias V, Krause TR and Whitlock C (2015) Complex response of white pines to past environmental variability increases understanding of future vulnerability. *PLoS One* 10(4). DOI: 10.1371/journal.pone.0124439.

International Tree-Ring Data Bank (2019) Available at: https://www.ncdc.noaa.gov/data-access/paleoclimatology-data/datasets/tree-ring (accessed 26 February 2019).

IPCC (2013) *Climate Change 2013: The Physical Science Basis: Contribution of Working Group I to the Fifth Assessment Report of the Intergovernmental Panel on Climate Change*. Cambridge; New York: Cambridge University Press.

Jones PD, Briffa KR, Barnett TP et al. (1998) High-resolution palaeoclimatic records for the last millennium: Interpretation, integration and comparison with General Circulation Model control-run temperatures. *The Holocene* 8(4): 455–471.

Kauppi P and Posch M (1985) Sensitivity of boreal forests to possible climatic warming. *Climatic Change* 7(1): 45–54.

King JC (2014) NOAA/WDS Paleoclimatology – King – Mount Washburn – PIAL – ITRDB WY050. *NOAA National Centers for Environmental Information*. Available at: https://doi.org/10.25921/kcje-x766 (accessed 14 September 2017).

Kipfmueller KF (2008) Reconstructed summer temperature in the northern Rocky Mountains Wilderness, USA. *Quaternary Research* 70: 173–187.

Körner C (2003) *Alpine Plant Life: Functional Plant Ecology of High Mountain Ecosystems*. Berlin; New York: Springer.

Krause TR, Lu Y, Whitlock C et al. (2015) Patterns of terrestrial and limnologic development in the northern Greater Yellowstone Ecosystem (USA) during the late-glacial/early-Holocene transition. *Palaeogeography Palaeoclimatology Palaeoecology* 422: 46–56.

Krause TR and Whitlock C (2013) Climate and vegetation change during the late-glacial/Early-Holocene transition inferred from multiple proxy records from Blacktail Pond, Yellowstone National Park, USA. *Quaternary Research* 79(3): 391–402.

Lageson DR and Spearing DR (1991) *Roadside Geology of Wyoming*. Missoula, MT: Mountain Press Publishing Company.

LaMarche VC (1973) Holocene climatic variations inferred from treeline fluctuations in the White Mountains, California. *Quaternary Research* 3(4): 632–660.

LaMarche VC and Mooney HA (1967) Altithermal timberline advance in western United States. *Nature* 213(5080): 980–982.

LaMarche VC and Mooney HA (1972) Recent climatic change and development of the bristlecone pine (P. longaeva Bailey) krummholz zone, Mt. Washington, Nevada. *Arctic and Alpine Research* 4(1): 61–72.

Larsson (2014) CooRecorder and Cdendro programs of the CooRecorder/Cdendropackage version 7.7. Available at: http://www.cybis.se/forfun/dendro/ (accessed 13 January 2020).

Leung LR, Qian Y, Bian X et al. (2004) Mid-century ensemble regional climate change scenarios for the western United States. *Climatic Change* 62(1–3): 75–113.

Lloyd AH and Graumlich LJ (1997) Holocene dynamics of treeline forests in the Sierra Nevada. *Ecology* 78: 1199–1210.

Luckman BH (2000) The Little Ice Age in the Canadian rockies. *Geomorphology* 32(3–4): 357–384.

Luckman BH, Jozsa LA and Murphy PJ (1984) Living seven-hundred-year-old Picea engelmannii and Pinus albicaulis in the Canadian Rockies. *Arctic and Alpine Research* 16(4): 419–422.

Luckman BH and Wilson RJS (2005) Summer temperatures in the Canadian Rockies during the last millennium: A revised record. *Climate Dynamics* 24: 131–144.

Lynch EA (1998) Origin of a park-forest vegetation mosaic in the Wind River Range, Wyoming. *Ecology* 79: 1320–1338.

MacDonald GM, Szeicz JM, Claricoates J et al. (1998) Response of the central Canadian treeline to recent climatic changes. *Annals of the Association of American Geographers* 88(2): 183–208.

MacFarlane WW, Logan JA and Kern WR (2013) An innovative aerial assessment of Greater Yellowstone Ecosystem mountain pine beetle-caused whitebark pine mortality. *Ecological Applications* 23(2): 421–437.

Mann ME, Fuentes JD and Rutherford S (2012) Underestimation of volcanic cooling in tree-ring-based reconstructions of hemispheric temperatures. *Nature Geoscience* 5(3): 202–205.

Mann ME, Zhang ZH, Hughes MK et al. (2008) Proxy-based reconstructions of hemispheric and global surface temperature variations over the past two millennia. *Proceedings of the National Academy of Sciences of the United States of America* 105: 13252–13257.

Mann ME, Zhang ZH, Rutherford S et al. (2009) Global signatures and dynamical origins of the Little Ice Age and Medieval Climate Anomaly. *Science* 326: 1256–1260.

Marcott SA, Fountain AG, O'Connor JE et al. (2009) A latest Pleistocene and Holocene glacial history and paleoclimate reconstruction at Three Sisters and Broken Top Volcanoes, Oregon, USA. *Quaternary Research* 71(2): 181–189.

McCarroll D, Pettigrew E, Luckman A et al. (2002) Blue reflectance provides a surrogate for latewood density of high-latitude pine tree rings. *Arctic, Antarctic, and Alpine Research* 34(4): 450–453.

Meko D (1997) Dendroclimatic reconstruction with time varying predictor subsets of tree indices. *Journal of Climate* 10(4): 687–696.

Melvin TM and Briffa KR (2008) A “signal-free” approach to dendroclimatic standardization. *Dendrochronologia* 26(2): 71–86.

Mensing S, Korfmacher J, Minckley T et al. (2012) A 15,000-year record of vegetation and climate change from a treeline lake in the Rocky Mountains, Wyoming, USA. *The Holocene* 22(7): 739–748.

Meyer GA, Wells SG, Balling RC Jr et al. (1992) Response of alluvial systems to fire and climate change in Yellowstone National Park. *Nature* 357(6374): 147–150.

Michaelsen J (1987) Cross-validation in statistical climate forecast models. *Journal of Climate and Applied Meteorology* 26(11): 1589–1600.

Morgan C, Losey A and Trout L (2014) Late-Holocene paleoclimate and treeline fluctuation in Wyoming’s Wind River Range, USA. *The Holocene* 24(2): 209–219.

Mote PW (2006) Climate-driven variability and trends in mountain snowpack in western North America. *Journal of Climate* 19(23): 6209–6220.

Mountain Research Initiative EDW Working Group (2015) Elevation-dependent warming in mountain regions of the world. *Nature Climate Change* 5: 424–430.

Osborn G and Gerloff L (1997) Latest Pleistocene and Early Holocene fluctuations of glaciers in the Canadian and Northern American Rockies. *Quaternary International* 38: 7–19.

Palmer WC (1965) *Meteorological Drought*, Vol. 30. Washington, DC: US Department of Commerce, Weather Bureau.

Perkins DL and Swetnam TW (1996) A dendroecological assessment of whitebark pine in the Sawtooth–Salmon River region, Idaho. *Canadian Journal of Forest Research* 26(12): 2123–2133.

Pierce JL, Meyer GA and Timothy Jull AJ (2004) Fire-induced erosion and millennial-scale climate change in northern ponderosa pine forests. *Nature* 432: 87–90.

Pyatt JC, Tomback DF, Blakeslee SC et al. (2016) The importance of conifers for facilitation at treeline: Comparing biophysical characteristics of leeward microsites in whitebark pine communities. *Arctic, Antarctic, and Alpine Research* 48(2): 427–444.

Reid RW, Whitney HS and Watson JA (1967) Reactions of lodgepole pine to attack by Dendroctonus ponderosae Hopkins and blue stain fungi. *Canadian Journal of Botany* 45: 1115–1126.

Reinemann SA, Porinchu DF, MacDonald GM et al. (2014) A 2000-yr reconstruction of air temperature in the Great Basin of the United States with specific reference to the Medieval Climatic Anomaly. *Quaternary Research* 82: 309–317.

Resler LM, Butler DR and Malanson GP (2005) Topographic shelter and conifer establishment and mortality in an alpine environment, Glacier National Park, Montana. *Physical Geography* 26(2): 112–125.

Resler LM and Tomback DF (2008) Blister rust prevalence in krummholz whitebark pine: Implications for treeline dynamics, Northern Rocky Mountains, Montana, U.S.A. *Arctic, Antarctic, and Alpine Research* 40: 161–170.

Rochner ML (2019) *Tree-ring evidence of climate and environmental change, Beartooth Mountains, Wyoming, U.S.A*. PhD Thesis, University of Tennessee, Knoxville, TN.

Rose R, Chachulski C and Haase D (1996) *Propagation of Pacific Northwest Native Plants: A Manual*, vol. 2, 1st edn. Corvallis, OR: Nursery Technology Cooperative, Oregon State University, pp.205–206.

Rossi S, Deslauriers A, Griçar J et al. (2008) Critical temperatures for xylogenesis in conifers of cold climates. *Global Ecology and Biogeography* 17(6): 696–707.

Salzer MW, Bunn AG, Graham NE et al. (2014) Five millennia of paleotemperature from tree-rings in the Great basin, USA. *Climate Dynamics: Observational, Theoretical and* 42(5–6): 1517–1526.

Salzer MW and Kipfmueller KF (2005) Reconstructed temperature and precipitation on a millennial timescale from tree-rings in the southern Colorado Plateau, USA. *Climatic Change* 70(3): 465–487.

Schweingruber FH, Eckstein D, Serre-Bachet F et al. (1990) Identification, presentation and interpretation of event years and pointer years in dendrochronology. *Dendrochronologia* 8: 9–38.

Schwörer C, Gavin DG, Walker IR et al. (2017) Holocene tree line changes in the Canadian Cordillera are controlled by climate and topography. *Journal of Biogeography* 44(5): 1148–1159.

Scuderi LA (1987) Late-Holocene upper timberline variation in the southern Sierra Nevada. *Nature* 325(6101): 242–244.

Sepulveda AJ, Tercek MT, Al-Chokhachy R et al. (2015) The shifting climate portfolio of the Greater Yellowstone Area. *PLoS One* 10(12): e0145060.

Shuman B (2012) Recent Wyoming temperature trends, their drivers, and impacts in a 14,000-year context. *Climatic Change* 112: 429–447.

Smith WK, Germino MJ, Johnson DM et al. (2009) The altitude of alpine treeline: A bellwether of climate change effects. *The Botanical Review* 75(2): 163–190.

Solheim H (1995) Early stages of blue-stain fungus invasion of lodgepole pine sapwood following mountain pine beetle attack. *Canadian Journal of Botany* 73(1): 70–74.

Steele R, Cooper SV, Ondov DM et al. (1983) Forest habitat types of eastern Idaho-western Wyoming. General Technical Report INT-144, US Department of Agriculture, Forest Service, Intermountain Forest and Range Experiment Station, Ogden, UT, July.

Stine S (1994) Extreme and persistent drought in California and Patagonia during mediaeval time. *Nature* 369(6481): 546–549.

Stokes MA and Smiley TL (1996) *An Introduction to Tree-Ring Dating*. Tucson, AZ: University of Arizona Press, p.73.

Tomback DF, Arno SF and Keane RE (2001) The compelling case for management intervention. In: Tomback DF, Arno SF and Keane RE (eds) *Whitebark Pine Communities: Ecology and Restoration*. Washington, DC: Island Press, pp.3–28.

Tomback DF, Resler LM, Keane RE et al. (2016) Community structure, biodiversity, and ecosystem services in treeline whitebark pine communities: Potential impacts from a non-native pathogen. *Forests* 7(12): 21.

Trouet V, Diaz HF, Wahl ER et al. (2013) A 1500-year reconstruction of annual mean temperature for temperate North America on decadal-to-multidecadal time scales. *Environmental Research Letters* 8(2): 024008.

Trouet V and Van Oldenborgh GJ (2013) KNMI Climate Explorer: A web-based research tool for high-resolution paleoclimatology. *Tree-Ring Research* 69(1): 3–13.

USDA (2013) Engelmann Spruce plant guide. USDA NRCS National Plant Data Center & the Biota of North America Program. Available at: https://plants.usda.gov/plantguide/pdf/pg_pien.pdf (accessed 26 October 2018).

Van der Maaten-Theunissen M, Van der Maaten E and Bouriaud O (2015) pointRes: An R package to analyze pointer years and components of resilience. *Dendrochronologia* 35: 34–38.

Vinod HD and López-de-Lacalle J (2009) Maximum entropy bootstrap for time series: ThemebootRPackage. *Journal of Statistical Software* 29(5): 1–19.

Wagner S and Zorita E (2005) The influence of volcanic, solar and CO2 forcing on the temperatures in the Dalton Minimum (1790–1830): A model study. *Climate Dynamics* 25(2–3): 205–218.

Wanner H, Beer J, Bütikofer J et al. (2008) Mid- to late-Holocene climate change: An overview. *Quaternary Science Reviews* 27: 1791–1828.

Weaver T (2001) Whitebark pine and its environment. In: Tomback DF, Arno SF and Keane RE (eds) *Whitebark Pine Communities: Ecology and Restoration*. Washington, DC: Island Press, pp.41–73.

Westerling AL, Hidalgo HG, Cayan DR et al. (2006) Warming and earlier spring increase western US forest wildfire activity. *Science* 313(5789): 940–943.

Westerling AL, Turner MG, Smithwick EAH et al. (2011) Continued warming could transform Greater Yellowstone fire regimes by mid-21st century. *Proceedings of the National Academy of Sciences* 108(32): 13165–13170.

Whitlock C (1993) Postglacial vegetation and climate of Grand Teton and southern Yellowstone National Parks. *Ecological Monographs* 63(2): 173–198.

Whitney HS (1971) Association of Dendroctonus ponderosae (Coleoptera: Scolytidae) with blue stain fungi and yeasts during brood development in lodgepole pine. *Canadian Journal of Entomology* 103: 1495–1503.

Wigley TML, Briffa KR and Jones PD (1984) On the average value of correlated time series, with applications in dendroclimatology and hydrometeorology. *Journal of Climate and Applied Meteorology* 23(2): 201–213.

Wiles GC, D'Arrigo RD, Villalba R et al. (2004) Century-scale solar variability and Alaskan temperature change over the past millennium. *Geophysical Research Letters* 31(15): L15203.

Wilson R, Anchukaitis K, Briffa KR et al. (2016) Last millennium northern hemisphere summer temperatures from tree rings: Part I: The long term context. *Quaternary Science Reviews* 134: 1–18.

Wilson R, Rao R, Rydval M et al. (2014) Blue Intensity for dendroclimatology: The BC blues: A case study from British Columbia, Canada. *The Holocene* 24(11): 1428–1438.